Research Square

Preprints are preliminary reports that have not undergone peer review.
They should not be considered conclusive, used to inform clinical practice,
or referenced by the media as validated information.

Unveiling the structural and functional specialization of the heart in the stingless bee Melipona quadrifasciata

Gustavo Martins

gmartins@ufv.br

Universidade Federal de Viçosa

Pedro Vilhete

Universidade Federal de Viçosa

Rhiala Albergaria

Universidade Federal de Viçosa

Samira Ravaiano

Universidade Federal de Viçosa

Article

Keywords:

Posted Date: November 23rd, 2026

DOI: https://doi.org/10.21203/rs.3.rs-11568859/v1

License: This work is licensed under a Creative Commons Attribution 4.0 International License.
Read Full License

Additional Declarations: No competing interests reported.

Unveiling the structural and functional specialization of the heart in the stingless bee *Melipona quadrifasciata*

Gustavo Ferreira Martins[a*], Pedro Emanuel Costa Vilhete[a], Rhiala Gomes Albergaria[b], Samira Veiga Ravaiano[b]

[a] Departamento de Biologia Geral, Universidade Federal de Viçosa, 36570-000, Viçosa, MG, Brazil

[b] Departamento de Entomologia, Universidade Federal de Viçosa, 36570-000, Viçosa, MG, Brazil

* Corresponding author: gmartins@ufv.br

Abstract

Stingless bees are highly diverse and ecologically important pollinators, yet their circulatory system remains poorly characterized. Here, we provide a comprehensive characterization of the heart of the stingless bee *Melipona quadrifasciata* using complementary techniques. In adult bees, the heart is a dorsal muscular tube comprising six serially arranged chambers. Its posterior region forms a bulbous dilation containing two chambers, followed anteriorly by four narrower chambers. All five pairs of ostia are incurrent and form valves through ostial lips that exhibit subcellular features consistent with contractile activity. A complex apparatus comprising alary muscles and their ramifications forms the dorsal diaphragm, which delimits the pericardial sinus. The posterior bulb has a reinforced muscular wall and a longitudinal muscle layer formed by reoriented cardiomyocytes that closes and supports its blind posterior end. This bulb is notable from a comparative perspective because a similar organization occurs in Meliponini and some solitary bees but appears to be absent in other eusocial bees. The robust muscular and valvar specialization of the posterior bulb may also contribute to the circulatory demands associated with the diverse and energetically demanding activities. These findings expand the understanding of stingless bee circulation and provide a structural framework for future functional studies.

Introduction

The insect circulatory system is an open system in which the hemolymph circulates through the hemocoel and is propelled by specialized pulsatile organs, most notably the dorsal vessel. The dorsal vessel is a tubular, linear organ that extends along the length of the body and functions as the primary structure responsible for hemolymph circulation. It is divided into two regions: the aorta, which extends through the thorax and head, and the heart, the contractile portion located in the abdomen.[1–3] In addition to hemolymph circulation, the circulatory system contributes to immunity, homeostasis, temperature regulation, gas exchange, and the transport of hormones and other signaling molecules, thereby integrating physiological processes throughout the organism.[4]

The heart is composed of multinucleated, striated muscle cells (cardiomyocytes) arranged in a helical or circular pattern.[2,5] It can be closed or opened at its posterior end, depending on the insect order; and possess paired lateral openings known as ostia. These ostia occur in pairs and in most cases allow the entry of hemolymph into the heart lumen, thereby functioning as incurrent ostia. Moreover, excurrent ostia, which allow the outflow of hemolymph, are also present in the hearts of certain insect groups, including Orthoptera, Thysanura, and Plecoptera.[1,2]

Several cell types are associated with the heart, including alary muscles, pericardial cells, and hemocytes (immune system cells). The alary muscles consist of paired muscle bundles that originate from the insect integument. These bundles branch and function to support the heart while also assisting in cardiac movements.[1,6–8] Pericardial cells are located along the lateral sides of the heart and may occur either as individual cells or in clusters. They contribute to hemolymph filtration and are therefore also referred to as nephrocytes.[1,2,6,9] Hemocytes can also be observed adjacently to the heart, where they accumulate primarily around the ostia.[10]

Cardiac morphology has been characterized across several insect groups, particularly in mosquitoes,[7,8,11,12] while *Drosophila* has emerged as a major model for elucidating the structure and function of the insect heart.[6,13–15] The cardiac structure of many other insect groups remains poorly characterized or largely unresolved. Bees, for example, remain comparatively understudied in this regard.

Bees exhibit a remarkable diversity of social organization, ranging from solitary species to highly eusocial forms. Among eusocial bees, the honey bee *Apis mellifera* is widely distributed worldwide and is of major ecological and economic importance.[16] Despite their ecological significance and complex biology, the cardiac system of bees remains understudied.[17]

Bees are highly active organisms, with intense flight activity associated particularly with foraging and nest defense, placing substantial demands on their circulatory system. Accordingly, the ecological diversity of bees also be reflected in the morphology of their cardiac system. To date, one of the earliest descriptions of the gross morphology of the bee heart was provided by Wille,[17] who documented interspecific variation among 101 species of adult bees. In some species, including stingless bees (Meliponini) and orchid bees (Euglossini), a bulbous or dilated region is present at the posterior end of the abdomen and corresponds to two distinct cardiac chambers, which are absent in bumble bees and honey bees.[17]

Stingless bees comprise more than 500 described highly eusocial species distributed predominantly across tropical regions. They live in complex societies in which colony activities are divided among different castes.[16] Brazil harbors one of the world's richest stingless bee faunas, with more than 250 species recorded. The genus *Melipona* is widely distributed throughout Brazil, and *Melipona quadrifasciata* Lepeletier, 1836, commonly known as "mandaçaia", is an important pollinator of tropical and subtropical plant species.[18,19] *M. quadrifasciata* comprises an important model for biological studies of stingless bees, owing to its ecological relevance, well-characterized biology, and suitability for laboratory-based research.

Species of *Melipona* are highly active flyers, capable of traveling nearly three kilometers in search of resources,[20] while carrying substantial loads, including pollen, mud, and plant materials on their corbiculae and nectar in the crop. Workers also contribute to colony hygiene by removing waste from the nest, including larval and adult corpses. In addition, foragers of this genus can perform buzzing, a behavior involving rapid movements of the thoracic flight muscles that generate high-frequency vibrations and is associated with pollen collection, nest defense, and colony maintenance.[21–23] These demanding activities

impose substantial physiological requirements on the circulatory system, which must support the intense metabolic demands associated with sustained and energetically costly flight.

In the present study, the heart of adult *M. quadrifasciata* was characterized in detail, with particular emphasis on its posterior region, a previously undescribed and structurally specialized dilated region or bulb comprising two cardiac chambers separated by a valvar structure. The structural organization and potential functional specialization of this region, including the muscular arrangement, ostial valves, and associated tissues, were discussed. This specialized cardiac region was characterized using complementary microscopy approaches and synchrotron radiation micro-computed tomography (SR-microCT). The characterization focused primarily on foragers, whereas observations from queens and males were used to complement the analysis.

Methods

Bees

Bees were collected from four *M. quadrifasciata* colonies maintained in rational hive boxes at the apiary of the Universidade Federal de Viçosa, Viçosa, Minas Gerais, Brazil, and from two colonies maintained at a private meliponary in rural Coimbra, Minas Gerais, Brazil. Foragers, typically 25 days old or older,[24] were captured in glass vials at the colony entrance upon returning from foraging activity.

For the collection of queens (2-5 days old), brood combs were maintained in the insectary of the Departamento de Biologia Geral (UFV), at 28 ± 3 °C, 75 ± 10% relative humidity, and a 12-h photoperiod. Brood combs were placed in Petri dishes lined with filter paper and provided with a honey solution (50% water and *A. mellifera* honey) until adult emergence. Brood cell cappings were manually removed with forceps to facilitate adult emergence.

Males were collected either while flying near colonies or as newly emerged individuals inside colonies or in brood combs. Newly emerged males collected from colonies or brood combs were maintained individually in Petri dishes with food. These males were considered to have reached the developmental stage at which males of the genus *Melipona* are expected to acquire flight capability, which occurs at approximately 18 days of age.[25]

Bees were cold-anesthetized at 4°C and dissected in phosphate-buffered saline (PBS; 0.1 M, pH 7.2). The abdomen was opened by making lateral incisions through the pleurae using micro-scissors. The ventral abdominal integument was then removed, and the visceral organs were carefully removed to expose the heart within the body cavity. Depending on the analysis, the heart was examined either in isolation or attached to the abdominal integument. In the latter preparations, only the portion of the integument directly overlying the heart was retained, while the lateral regions were removed using micro-scissors. These preparations were used for light microscopy and scanning electron microscopy. For fluorescence microscopy, confocal laser scanning microscopy, and transmission electron microscopy, the heart was carefully removed from the integument.

Samples intended for light, fluorescence, and confocal microscopy were fixed in Zamboni's fixative (picric acid and formaldehyde; pH 7.3). Samples prepared for electron microscopies were fixed in 2.5% glutaraldehyde in 0.1 M sodium cacodylate buffer (pH 7.3).

In Vivo filming

For photographs and video recordings of cardiac activity, live and anesthetized foragers were dissected (at least 10). Bees was positioned with the ventral side facing upward and secured to a paraffin wax plate using two entomological pins: one inserted through the thorax and the other through the distal end of the abdomen, which was gently extended and fixed in position with the pin. The abdomen was opened, and the visceral organs were removed to expose the heart. Cardiac activity was recorded using a Canon EOS Rebel T7i camera coupled to a Zeiss Stemi 2000-C stereomicroscope through an appropriate camera adapter.

Synchrotron radiation micro-computed tomography (SR-microCT)

The abdomen of one anesthetized forager was separated from the remainder of the body using a micro-scissor and transferred to a microtube containing 100% ethanol. The microtube was then placed in a vacuum chamber for approximately 10 min to remove air bubbles trapped within the sample. A mixture of ethanol and triturated agar-agar was

subsequently introduced into the same microtube to immobilize and stabilize the specimen during scanning.

The specimen was imaged using synchrotron radiation micro-computed tomography (SR-microCT) at the MOGNO (Micro and Nano Tomography) beamline of the Brazilian Synchrotron Light Laboratory (LNLS), Centro Nacional de Pesquisa em Energia e Materiais (CNPEM), Campinas, São Paulo, Brazil. The MOGNO beamline operates over an energy range of 22–39 keV, with a hard X-ray energy of 67.5 keV.

Segmentation and initial visualization of the tomographic dataset were performed using 3D Slicer (version 5.10.0). Segment interpolation was subsequently performed using the open-source platform BIOMEDISA[26] by applying smart distance-map interpolation between manually annotated control slices to delineate the regions of interest. The resulting three-dimensional mesh models were exported to Blender (version 5.2.2). The time-series animation was rendered and exported as an uncompressed image sequence (PNG format, 1920 X 1080 pixels, 8-bit per channel, 24 frames per second). The resulting image stack was imported into Fiji/ImageJ software (v. 1.54p). For spatial noise reduction and file size optimization, a 2 x 2 spatial binning (local averaging method) was applied while maintaining the original temporal sampling rate intact. The processed stack was subsequently compiled and exported as an AVI video file (JPEG compression, 24 fps).

Light microscopy

Fixed forager organs, either attached to or isolated from the body wall, were washed in PBS and dehydrated through a graded ethanol series (70-100%). Dehydrated samples (n = 5) were cleared in xylene for whole-mount preparations. A separate set of samples (at least 20) was subsequently embedded in historesin (Leica Microsystems, Heidelberg, Mannheim, Germany) for histological analysis. Infiltration was performed using a 2:1 mixture of 100% ethanol and resin for 1 h, followed by a 1:1 mixture for an additional 1 h and pure resin for 24 h, according to the manufacturer's protocol.

The samples were positioned in plastic molds in different orientations and maintained under vacuum until polymerization. Sections 3-5 µm thick were obtained using glass knives mounted on a microtome (Reichert Jung 2050, Nussloch, Germany). The sections were

mounted on glass slides, stained with toluidine blue, and coverslipped using Eukitt mounting medium (Fluka, St. Louis, MO, USA). The preparations were photographed using an Olympus Q-Color 3 digital camera coupled to an Olympus BX60 light microscope or an Opticam EOPT20003_ISPor digital camera coupled to an Opticam O600R light microscope.

Scanning electron microscopy

Hearts attached in the integument from foragers and males (n = 5 per group) were fixed in 2.5% glutaraldehyde in 0.1 M cacodylate buffer (pH 7.2), washed with PBS, dehydrated through a graded ethanol series, and dried using a Balzers CPD 030 critical-point dryer. The dried specimens were mounted on aluminum stubs and sputter-coated with gold using a Quorum Q150R S sputter coater. Images were acquired using a LEO VP1430 scanning electron microscope at the Núcleo de Microscopia e Microanálises, Universidade Federal de Viçosa (NMM/UFV). Fixed isolated hearts from foragers (n = 5) were mounted on carbon tape attached to stubs and carefully opened to expose the organ lumen, metalized and examined.

Fluorescence microscopy and confocal laser scanning microscopy

Fixed hearts from foragers (n = 5) were incubated with Phalloidin-FITC (Sigma-Aldrich, Sigma-Aldrich Brasil Ltda.) at a 1:250 dilution for 1 h 20 min in the dark and washed three times with PBS for 5 min each. The preparations were then mounted and examined and whole mounts were photographed using the Opticam fluorescence microscope. The same preparations were subsequently examined and photographed using a Zeiss LSM 900 confocal laser scanning microscope NMM/UFV.

A second set of isolated and fixed hearts from foragers, queens, and males (n = 5 per class) was washed in 0.1% Triton X-100 for 30 min. The samples were then incubated with Phalloidin-FITC at a 1:500 dilution and washed. Subsequently, the samples were incubated with TO-PRO-3 (Life Technologies) at a 1:900 dilution for 30 min in the dark and washed three times with PBS for 10 min each. After staining, the samples were mounted on histological slides using mowiol-based mounting medium. The specimens were analyzed and

photographed using a Zeiss LSM 510 Meta confocal laser scanning microscope at the NMM/UFV.

Transmission electron microscopy

After fixation, the posterior cardiac chambers of two foragers were isolated and post-fixed in 1% osmium tetroxide in 0.1 M sodium cacodylate buffer (pH 7.2) for 2 h, followed by rinsing in PBS. Samples were subsequently dehydrated in ethanol and infiltrated with LR White resin (London Resin Company Ltd., Berkshire, UK), using a 1:1 mixture of resin and 100% ethanol for 24 h. The samples were then transferred to pure resin and maintained for an additional 24 h.

Polymerization was performed in gelatin capsules (0.95 mL; Electron Microscopy Sciences-EMS, Hatfield, PA, USA) for 24 h at 60 °C. Ultrathin sections were obtained using an RMC PowerTome-X ultramicrotome and collected on copper grids (EMS). Semithin sections (1µm) were stained with toluidine blue in borax and mounted on glass slides and photographed. The thin sections (80-90 nm) were contrasted with 3% uranyl acetate and 0.2% lead citrate for 20 min each. Images were acquired using a Zeiss EM 109 transmission electron microscope at NMM/UFV.

Image processing and generative AI

When necessary, images were processed for clarity and presentation using Corel PHOTO-PAINT (CorelDRAW Graphics Suite, Corel Corporation, Ottawa, ON, Canada) or Adobe Photoshop (Adobe Inc., San Jose, CA, USA). Image processing was limited to assembling composite figures, removing non-informative background artifacts or noise, and making adjustments to brightness and contrast. These adjustments did not affect data interpretation.

Generative AI tools were used to assist with language editing and translation refinement. All AI-assisted text was thoroughly verified and revised by the authors, who take full responsibility for the final content.

Results

The heart of adult *M. quadrifasciata* workers, queens, and males is a translucent, muscular tube located dorsally along the abdominal midline, beneath the integument. It is curved, following the contour of the abdomen. The organ extends to the sixth abdominal segment and is absent from the seventh segment, which is the terminal visible abdominal segment in foragers. A layer of pericardial cells extends along the entire length of the heart, forming a continuous cellular barrier along its lateral surfaces and posterior end. The posterior end of the heart, corresponding to the distal portion, is dilated and forms a bulb-like structure (Figs. 1, 2).

The bulb comprises two cardiac chambers, whose boundary is externally marked by a pair of ostia. The proximal chamber, which is larger and longer than the distal chamber, is narrow anteriorly and broadens abruptly within the bulb, where it occupies a shorter portion of the chamber. The distal chamber is smaller, becoming flattened and narrower toward the posterior end of the bulb, where it terminates blindly (Figs. 1, 2, Sup. Videos 1-3).

In foragers of *M. quadrifasciata*, the heart comprises six cardiac chambers separated by five valves. The narrower portion of the heart comprises four complete chambers and the tapered portion of the first chamber within the bulb, with the four complete chambers separated by four valves. These chambers progressively decrease in width toward the anterior region of the abdomen. Near the abdominal-thoracic junction, the heart narrows further to form the aorta (Sup. Videos 1-3; Figs. 2, 5F), which extends into the thorax but was not examined in the present study. Slight lateral dilations occur at the beginning of each chamber in the narrower portion of the heart, corresponding to the valvar regions and coinciding with the ostia, which form five pairs of lateral openings between adjacent chambers (Figs. 1, 2, 3E, Sup. Videos 1, 3).

The heart wall has a striated surface and consists predominantly of muscular tissue formed by circular muscle fibers (Fig. 4). At the posterior end of the bulb, the most distal circular muscle fibers originate dorsally, extend around and close the posterior extremity, and continue onto the ventral surface, where they form a longitudinal muscle layer (Figs. 1A, 4C, 4E, 5A, 8A). At this region, where the longitudinal fibers converge to close the organ, the muscle fibers overlap (Fig. 7A). In beating hearts, this layer becomes barely discernible during cardiac relaxation (diastole), revealing the predominance of the circular arrangement

of muscle fibers in the terminal chamber of the bulb and making the posterior end of the heart appear open (Fig. 1D). The longitudinal layer becomes progressively thinner toward the anterior region of the bulb (Figs. 1A-C, 4C, 8A). On the dorsal wall of the bulb, circular muscle fibers are also visible; however, the median region of the bulb appears smooth on both the external and luminal surfaces, although circular fibers are clearly observed in histological sections (Figs. 1C, 4A, 8B).

The multinucleated cardiomyocytes of foragers are arranged side by side in two semicircular rows, forming a single-cell-thick tubular heart wall. Their close apposition produces an irregularly undulating inner surface of the heart wall, with alternating ridges and depressions (Figs. 4, 5A, 5B). The cardiomyocytes are joined at two points, one along the dorsal surface and the other along the ventral surface, except at the posterior end of the last cardiac chamber in the bulb. The insertion sites of the cardiomyocytes appear as constricted regions extending throughout the organ and beginning at the transition between the bulb and the narrow region. These insertion sites are observed as two continuous lines extending along the organ and lacking phalloidin-FITC labeling (Figs. 4B, 5B, 5C, 8B-D). Cardiomyocytes form a thick muscular wall in the bulb region, exhibiting Z-line-like arrangements characteristic of sarcomeres and numerous mitochondria (Figs. 9A, 10A).

The ostia of *M. quadrifasciata* are incurrent openings through which hemolymph enters the lumen of the dorsal vessel. They open and close during the cardiac cycle (Sup. Video 4). Cardiomyocytes at the ostial margins extend into the cardiac lumen, forming long, slender ostial lips (Figs. 4D, 5E, 6, 7; Sup. Video 3). These lips form valve-like flaps oriented toward the anterior end of the body, with each pair constituting an intercameral valve between adjacent cardiac chambers (Sup. Videos 2, 3). Valves in the narrower region of the heart also exhibit filiform projections extending from the distal ends of the ostial lips, detectable only by SR-microCT (Figs. 6, 7).

During *in vivo* observations of dissected foragers, the bulb filled with hemolymph through its ostia during relaxation (diastole) and expelled it during the contraction (systole) toward the anterior region of the body, into the narrower portion of the heart. The bulb filled during relaxation, followed by one, two, or three successive rapid contractions in our observations. Notably, the ostia in the bulb were larger than those observed in the narrower portion of the heart (Sup. Video 3).

The ostial lips are flexible structures that expand anteriorly during cardiac contraction, opening the valve and allowing hemolymph to pass into the subsequent chamber, and retract during cardiac relaxation (Sup. Video 4), consistent with the cytoskeletal organization of these cells. The lips exhibit ultrastructural features of contractile muscle cells, including sarcomeres and numerous mitochondria (Figs. 9B, C), and their contractile nature is further supported by phalloidin-FITC labeling (Fig. 5E). The valve separating the two posterior chambers is characterized by exceptionally long ostial lips (Figs. 4D, 6G, 6H, 7A, 7C). Each lip is composed of multiple cells that progressively become thinner toward its distal end (Figs. 7C-E).

The ventral surface of the heart is associated with the dorsal diaphragm, which demarcates the pericardial sinus from the surrounding body cavity (Figs. 3C; 6A-D; 10; Sup. Video 3). The diaphragm is composed of alary muscles, their branches and pericardial cells. The alary muscles are anchored to the tergites and extend toward the heart as bundles of muscle fibers, which give rise to branches that form a continuous tissue layer beneath the muscular wall. This layer consists of elongated, flattened extensions with scant cytoplasm and nuclei, providing a supporting surface on which the heart rests. These branches are irregular in shape and separated by wide intercellular spaces, with indistinct cell boundaries. (Figs. 3, 6A, 6B, 10; Sup. Video 3).

Another group of very fine branches originating from the alary fibers extends along the heart wall and attaches to the integument, anchoring the organ to the dorsal body wall. Similarly, very fine suspensory structures connect the posterior end of the bulb to the integument, forming a radial arrangement around the bulb (Figs. 3, 10B). The origin of these latter structures from the alary fibers could not be determined. Light and electron microscopy revealed no discernible cellular structures within these elements, suggesting that they are extracellular matrix fibers, as described in *Drosophila melanogaster*.[14,15] Together, the alary muscles and their ramifications, pericardial cells, and putative extracellular matrix fibers form a complex suspensory apparatus that maintains the heart along the abdominal midline.

The pericardial cells have abundant cytoplasm and relatively small nuclei in relation to cell size, with relatively decondensed chromatin and a prominent nucleolus. They are commonly grouped into cords associated with the alary fiber. These cells exhibit membrane

invaginations or canaliculi, as well as numerous structures associated with endocytosis (Fig. 11).

Discussion

Stingless bees comprise a highly diverse group of pollinators of ecological and economic importance in tropical and subtropical regions. They exhibit several biological and morphological adaptations that distinguish them from bumble bees and honey bees, including the loss of the functional sting.[16] Despite these distinctive features, substantial gaps remain in our understanding of their circulatory system, particularly the organization and function of the dorsal vessel, which in stingless bees includes a posterior bulb comprising two cardiac chambers.[17] Here, we provide a detailed characterization of the heart of *M. quadrifasciata*, a stingless bee widely distributed across Brazil, using complementary microscopy and microanalysis techniques to investigate its structural organization and dynamics. This integrative approach revealed previously undescribed structural features and provided insights into the functional specialization of the heart. The analyses focused primarily on foragers, whereas virgin queens and males were examined in selected analyses to provide complementary observations across castes and sexes. Although the heart was not characterized in equal detail across these groups, its general organization appeared broadly similar, including the presence of a distinct posterior dilation, or bulb, which was the primary focus of this study. These findings establish a framework for future comparative investigations of cardiac organization and function across bee species, castes, sexes, developmental stages, and physiological conditions.

In bees, the heart exhibits a progressive decrease in caliber from the posterior to the anterior region,[5,17,27] consistent with the general pattern of variation in caliber along the insect heart.[28] Within this overall gradient, however, the two posterior-most chambers are markedly wider, forming a bulbous dilation that terminates in a blind end in stingless bees, including *M. quadrifasciata*. A dilation involving the two posterior-most chambers of the dorsal vessel has been reported in Meliponini, a group of highly eusocial bees, as well as in some solitary bees, including orchid bees (Euglossini).[17,27] This feature occurs in Meliponini despite their closer phylogenetic relationship to Apini than to Euglossini.[29] Although the posterior region of the heart is also widened in Apini, it does not develop into a bulb as pronounced as that

found in Meliponini, raising questions about the evolutionary history and functional significance of this structural specialization in stingless bees. Orchid bees are characterized by vigorous flight activity and high metabolic demands associated with flight,[30,31] and this posterior dilation may be associated with meeting theses elevated energetic needs. The dilation may accommodate a greater volume of hemolymph and facilitate its propulsion toward the anterior region of the body in both stingless and orchid bees, while its larger caliber and reinforced muscular wall may contribute to increased contractile force.[17]

The insect heart is enclosed by a muscular wall and divided into sequentially arranged cardiac chambers. The circular arrangement of cardiomyocytes in *M. quadrifasciata* is similar to that reported in the stingless bee *Scaptotrigona postica*.[32] However, cardiomyocyte arrangement is not conserved across insects, and a helical organization of the cardiomyocytes has been described in several other insect species.[7,11,12,33–36] However, the implication of differences in cardiomyocyte arrangement among insects is still unknown. In bees, the junctions between cardiomyocyte ends have been described as being formed by an amorphous extracellular material considered part of the connective tissue,[37] whereas adherens junctions have been described in *D. melanogaster*.[38–40] Although adherens junctions were not resolved in the present study, their presence cannot be excluded.

The blind posterior end of the heart, associated with unidirectional hemolymph flow, has been considered an apomorphic feature of the insect circulatory system.[41] In *M. quadrifasciata*, the posterior bulb terminates in a blind end reinforced by longitudinal muscle fibers formed by cardiomyocytes that extend parallel to the vessel and overlap around its terminal region, forming a distinct bundle. This arrangement may provide mechanical support to the bulb and terminal cardiac chamber during contraction, potentially contributing to the anterior propulsion of hemolymph. To our knowledge, this longitudinal muscle arrangement has not previously been described in Hymenoptera and therefore represents a novel finding.

In *M. quadrifasciata*, the heart comprises six chambers associated with ostial valves. Each valve is formed by two pairs of elongated ostial lips, with one pair on each lateral-ventral side of the organ, and an ostium is present between each pair of lips. Five pairs of incurrent ostia have been reported in the abdominal heart of bees of Apidae.[5,17,37] During

diastole, the valves of *M. quadrifasciata* open to permit hemolymph entry, whereas during systole, contraction of the ostial lips closes the openings and prevents backflow.[6,12,14]

The ostial lips are inward projections of cardiomyocytes bordering the ostia and extend into the cardiac lumen.[17] In *M. quadrifasciata*, ostial lips are composed of contractile muscle cells, suggesting a myogenic component similar to that described in *D. melanogaster* and mosquitoes.[42,43] Moreover, ostial lip cells in the cardiac bulb of *M. quadrifasciata* exhibit ultrastructural features indicative of high cellular activity, including well-developed endoplasmic reticulum, consistent with active protein synthesis and maintenance of these specialized contractile cells.

The ostial lips between the chambers of the bulb are longer than those in the narrower anterior region of the heart of *M. quadrifasciata*. Their greater length may facilitate hemolymph transfer from the terminal chamber to the subsequent chamber during contraction while helping to limit backflow. The more robust ostial valves between the dilated chambers, together with the reinforced muscular wall and more developed dorsal diaphragm, may enhance the propulsive capacity of the bulb. The heart narrows abruptly at the antepenultimate cardiac chamber within the bulb and continues to decrease in caliber toward the thorax. Given this progressive reduction in cardiac caliber and the considerable distance hemolymph must travel along the dorsal vessel from the abdomen toward the head, sufficient contractile force and pressure generation within the bulb may be required to overcome resistance to flow and maintain forward hemolymph transport. The more robust ostial valves may be important in preventing backflow during this propulsive process.

The dorsal diaphragm of *M. quadrifasciata* is composed by alary fibers, pericardial cells and connective tissue and has been described in various insects.[1,4,41] In *M. quadrifasciata*, multiple layers of elongated branches extend from the alary fibers, forming a thick tissue layer. This structure forms a suspensory apparatus that supports the heart within the abdominal cavity.[5] The branches of the alary fibers contain relatively little cytoplasm and few organelles, consistent with a predominantly structural role.

An additional group of sparse fibrillar structures connects the dorsal surface of the heart of *M. quadrifasciata* to the overlying integument, providing further mechanical support. These structures, referred to here as extracellular matrix fibers, have also been described in *D. melanogaster*[14] and may correspond to structures termed suspensory cells in other insects.[2]

However, light and electron microscopy revealed no discernible cellular components in these structures in *M. quadrifasciata*, providing no evidence that they represent distinct cells. These fibers are arranged around the bulbous posterior region, including its blind end, and may contribute to its mechanical support. Together with other suspensory elements, they form an elaborate suspensory apparatus resembling that described in *A. mellifera*.[5]

Pericardial cells in *M. quadrifasciata* are grouped in cords surrounding the heart and are physically associated with branches of the alary muscles.[7,11,35,44] The cord-like arrangement observed in *M. quadrifasciata* is also consistent with that described in workers and queens of *S. postica*.[32,45] Invaginations of the pericardial cell membrane form canaliculi that increase the cell surface area in contact with the hemolymph, facilitating the uptake of compounds and contributing to their filtration function. The presence of numerous intracellular structures associated with these invaginations, including organelles characteristic of the endocytic pathway, further supports active uptake and intracellular processing of substances by these cells.[9,46] Because the organization and ultrastructural features of the pericardial cells observed here are consistent with previous descriptions in bees and other insects, and no distinctive features were identified in *M. quadrifasciata*, these cells are not discussed further.

The heart of *M. quadrifasciata* exhibits a structural specialization involving a posterior bulb comprising two serially arranged cardiac chambers and elongated intercameral ostial valves. Through complementary microscopy techniques and synchrotron radiation micro-computed tomography, this study provides a comprehensive morphological characterization of the heart and its associated structures. The presence of a posterior bulb with two chambers is particularly noteworthy from a comparative perspective, as a similar organization has been reported in Meliponini and in solitary bees, whereas it appears to be absent in eusocial Apidae such as honey bees and bumble bees.[5,17,27] This distribution raises the possibility that the two-chambered posterior bulb represents an ancestral condition that has been retained in Meliponini but secondarily lost in some lineages of eusocial bees. The evolutionary and functional significance of this contrasting pattern remains unclear and warrants further comparative investigation, particularly given the striking differences in social organization and behavioral complexity among bees.

The robust posterior bulb, its ostial valve, and their well-developed supporting structures may also be functionally relevant to the high energetic demands associated with the diverse activities performed by stingless bees, including sustained flight, resource transport, and complex behaviors such as buzzing. Thus, the pronounced structural development of the posterior cardiac region may be consistent with a circulatory system adapted to support the high metabolic demands associated with these activities. Finally, these findings expand the current understanding of the circulatory system of stingless bees and provide a morphological basis for future comparative, evolutionary, and functional studies.

Data availability

The original images and videos used in the current study are available from the corresponding author.

Acknowledgements

To Dr. Thomas van de Kamp (Institute for Photon Science and Synchrotron Radiation, Karlsruhe Institute of Technology, Germany) for his initial assistance with the microtomographic analyses. This research also used facilities of the Brazilian Synchrotron Light Laboratory (LNLS), part of the Centro Nacional de Pesquisa em Energia e Materiais (CNPEM). The MOGNO beamline staff are acknowledged for their assistance during the experiments (proposal 20262004). This research used facilities of the Núcleo de Microscopia e Microanálise at the Universidade Federal de Viçosa, Minas Gerais, Brazil. We thank the staff for providing access to the equipment and technical assistance during the ultrastructural analyses.

Funding

This work was supported by the Coordenação de Aperfeiçoamento de Pessoal de Nível Superior (CAPES) and the Conselho Nacional de Desenvolvimento Científico e Tecnológico (CNPq).

Author Contributions

G.F.M., P.E.C.V., and S.V.R. conceived the study. G.F.M., P.E.C.V., and S.V.R. designed the experiments. G.F.M., P.E.C.V., R.G.A., and S.V.R. performed the experiments. G.F.M., P.E.C.V., R.G.A., and S.V.R. analyzed the data. G.F.M., P.E.C.V. interpreted the results. G.F.M. and R.G.A prepared the figures. G.F.M. and P.E.C.V. drafted the manuscript. G.F.M., P.E.C.V. and R.G.A. edited, revised, and approved the final version of the manuscript. G.F.M. acquired funding and supervised the study.

Competing interests

The authors declare no competing interests.

Ethical approval

Not applicable

Conflict of interest

The author(s) declared that this work was conducted in the absence of any potential conflict of interest.

References

1. Klowden, M. J. *Physiological Systems in Insects* 2nd edn (Academic Press, 2007).

2. Chapman, R. F. *The Insects: Structure and Function* 5th edn (Cambridge Univ. Press, 2013).

3. Hillyer, J. F. Insect immunology and hematopoiesis. *Dev. Comp. Immunol.* **58**, 102–118 (2016). https://doi.org/10.1016/j.dci.2015.12.006

4. Hillyer, J. F. & Pass, G. The insect circulatory system: structure, function, and evolution. *Annu. Rev. Entomol.* **65**, 121–143 (2020). https://doi.org/10.1146/annurev-ento-011019-025003

5. Snodgrass, R. E. *Anatomy of the Honeybee* (Read Books Ltd, 2017).

6. Curtis, N. J., Ringo, J. M. & Dowse, H. B. Morphology of the pupal heart, adult heart and associated tissues in the fruit fly, *Drosophila melanogaster*. *J. Morphol.* **240**, 225–235 (1999). https://doi.org/10.1002/(SICI)1097-4687(199906)240:33.0.CO;2-V

519 7. Glenn, J. D., King, J. G. & Hillyer, J. F. Structural mechanics of the mosquito heart and
520 its function in bidirectional hemolymph transport. *J. Exp. Biol.* **213**, 541–550 (2010).
521 https://doi.org/10.1242/jeb.035014

522 8. Martins, G. F., Ramalho-Ortigão, J. M. & Pimenta, P. F. P. Morphological features of the
523 heart of six mosquito species as revealed by scanning electron microscopy. *Int. J. Trop. Insect*
524 *Sci.* **31**, 98–102 (2011). https://doi.org/10.1017/S1742758411000178

525 9. Rocha, V. C., da Silva, H. B., Barbosa, R. C. & Martins, G. F. Integrated morphological
526 analyses of *Cladomorphus phyllinus* and transcriptomic analysis of *Cladomorphus*
527 *trimariensis* provide insights into the cardiac morphophysiology of stick insects (Phasmida:
528 Phasmatidae). *Cell Tissue Res.* **405**, 1 (2026). https://doi.org/10.1007/s00441-026-04084-3

529 10. King, J. G. & Hillyer, J. F. Infection-induced interaction between the mosquito
530 circulatory and immune systems. *PLoS Pathog.* **8**, e1003058 (2012).
531 https://doi.org/10.1371/journal.ppat.1003058

532 11. Leódido, A. C. M., Ramalho-Ortigão, M. & Martins, G. F. The ultrastructure of the *Aedes*
533 *aegypti* heart. *Arthropod Struct. Dev.* **42**, 539–550 (2013).
534 https://doi.org/10.1016/j.asd.2013.09.005

535 12. League, G. P., Onuh, O. C. & Hillyer, J. F. Comparative structural and functional analysis
536 of the larval and adult dorsal vessel and its role in hemolymph circulation in the mosquito
537 *Anopheles gambiae*. *J. Exp. Biol.* **218**, 370–380 (2015). https://doi.org/10.1242/jeb.114942

538 13. Tao, Y. & Schulz, R. A. Heart development in *Drosophila*. *Semin. Cell Dev. Biol.* **18**, 3–
539 15 (2007). https://doi.org/10.1016/j.semcdb.2006.12.001

540 14. Lehmacher, C., Abeln, B. & Paululat, A. The ultrastructure of *Drosophila* heart cells.
541 *Arthropod Struct. Dev.* **41**, 459–474 (2012). https://doi.org/10.1016/j.asd.2012.02.002

542 15. Rotstein, B. & Paululat, A. On the morphology of the *Drosophila* heart. *J. Cardiovasc.*
543 *Dev. Dis.* **3**, 15 (2016). https://doi.org/10.3390/jcdd3020015

544 16. Michener, C. D. *The Bees of the World* 2nd edn (Johns Hopkins Univ. Press, 2007).

545 17. Wille, A. A comparative study of the dorsal vessels of bees. *Ann. Entomol. Soc. Am.* **51**,
546 538–546 (1958). https://doi.org/10.1093/aesa/51.6.538

547 18. Heard, T. A. The role of stingless bees in crop pollination. *Annu. Rev. Entomol.* **44**, 183–
548 206 (1999). https://doi.org/10.1146/annurev.ento.44.1.183

549 19. Silveira, F. A., Melo, G. A. R. & Almeida, E. A. B. *Abelhas Brasileiras: Sistemática e*
550 *Identificação* (IDM Composição e Arte, 2002).

20. Araújo, E. D., Costa, M., Chaud-Netto, J. & Fowler, H. G. Body size and flight distance in stingless bees (Hymenoptera: Meliponini): inference of flight range and possible ecological implications. *Braz. J. Biol.* **64**, 563–568 (2004). https://doi.org/10.1590/S1519-69842004000400003

21. Hrncir, M., Schorkopf, D. L. P., Schmidt, V. M., Zucchi, R. & Barth, F. G. The sound field generated by tethered stingless bees (*Melipona scutellaris*): inferences on its potential as a recruitment mechanism inside the hive. *J. Exp. Biol.* **211**, 686–698 (2008). https://doi.org/10.1242/jeb.013938

22. Hart, A. Waste management in the stingless bee *Melipona beecheii* Bennett (Hymenoptera: Apidae). *Sociobiology* **61**, 435–440 (2014). https://doi.org/10.13102/sociobiology.v61i4.435-440

23. Devkota, K. et al. The worker flow at the hive entrance predicts when nest cleaning is intensified in stingless bees. *Psyche* **2024**, 6659234 (2024). https://doi.org/10.1155/2024/6659234

24. Kerr, W. E., Carvalho, G. A. & Nascimento, V. A. *Abelha Uruçu: Biologia, Manejo e Conservação* (Fundação Acangau, 1996).

25. van Veen, J. W., Sommeijer, M. J. & Meeuwsen, F. Behaviour of drones in *Melipona* (Apidae, Meliponinae). *Insectes Soc.* **44**, 435–447 (1997).

26. Lösel, P. D. et al. Introducing Biomedisa as an open-source online platform for biomedical image segmentation. *Nat. Commun.* **11**, 5577 (2020). https://doi.org/10.1038/s41467-020-19303-w

27. Wille, A. Phylogenetic significance of an unusual African stingless bee, *Meliponula bocandei* (Spinola). *Rev. Biol. Trop.* **11**, 25–45 (1963). https://doi.org/10.15517/rev.biol.trop.1963.31135

28. Pass, G. et al. Phylogenetic relationships of the orders of Hexapoda: contributions from the circulatory organs for a morphological data matrix. *Arthropod Syst. Phylogeny* **64**, 165–203 (2006).

29. Hedtke, S. M., Patiny, S. & Danforth, B. N. The bee tree of life: a supermatrix approach to apoid phylogeny and biogeography. *BMC Evol. Biol.* **13**, 138 (2013). https://doi.org/10.1186/1471-2148-13-138

30. Suarez, R. K. et al. Energy metabolism in orchid bee flight muscles: carbohydrate fuels all. *J. Exp. Biol.* **208**, 3573–3579 (2005). https://doi.org/10.1242/jeb.01775

31. Wikelski, M. et al. Large-range movements of neotropical orchid bees observed via radio telemetry. *PLoS ONE* **5**, e10738 (2010). https://doi.org/10.1371/journal.pone.0010738

585 32. Poiani, S. B. & Cruz-Landim, C. Histologia e ultra-estrutura do vaso dorsal de
586 *Scaptotrigona postica* (Hymenoptera, Apidae) em operárias e rainhas de diferentes idades.
587 *Iheringia Sér. Zool.* **96**, 121–126 (2006). https://doi.org/10.1590/S0073-
588 47212006000100021

589 33. Wasserthal, L. T. & Wasserthal, W. Innervation of heart and alary muscles in *Sphinx*
590 *ligustri* L. (Lepidoptera). *Cell Tissue Res.* **184**, 467–486 (1977).

591 34. Locke, M. Secretion by insect heart muscle cell. *J. Insect Physiol.* **35**, 53–56 (1989).

592 35. Chiang, R. G., Chiang, J. A. & Davey, K. G. Morphology of the dorsal vessel in the
593 abdomen of the blood-feeding insect *Rhodnius prolixus*. *J. Morphol.* **204**, 9–23 (1990).
594 https://doi.org/10.1002/jmor.1052040103

595 36. Ejaz, A. & Lange, A. B. Peptidergic control of the heart of the stick insect, *Baculum*
596 *extradentatum*. *Peptides* **29**, 214–225 (2008). https://doi.org/10.1016/j.peptides.2007.07.036

597 37. Cruz-Landim, C. *Abelhas: Morfologia e Função de Sistemas* (Editora SciELO–Ed.
598 UNESP, 2009).

599 38. Medioni, C., Astier, M., Zmojdzian, M., Jagla, K. & Sémériva, M. Genetic control of cell
600 morphogenesis during *Drosophila melanogaster* cardiac tube formation. *J. Cell Biol.* **182**,
601 249–261 (2008). https://doi.org/10.1083/jcb.200801100

602 39. Wasserthal, L. T. Functional morphology of the heart and of a new cephalic pulsatile
603 organ in the blowfly *Calliphora vicina* (Diptera: Calliphoridae) and their roles in hemolymph
604 transport and tracheal ventilation. *Int. J. Insect Morphol. Embryol.* **28**, 111–129 (1999).
605 https://doi.org/10.1016/S0020-7322(99)00012-4

606 40. Bodmer, R. & Frasch, M. Genetic determination of *Drosophila* heart development. In
607 *Cellular and Molecular Biology of Muscle* (Academic Press, 1999).

608 41. Gereben-Krenn, B.-A. & Pass, G. Circulatory organs of abdominal appendages in
609 primitive insects (Hexapoda: Archaeognatha, Zygentoma and Ephemeroptera). *Acta Zool.*
610 **81**, 285–292 (2000). https://doi.org/10.1046/j.1463-6395.2000.00057.x

611 42. Lammers, K. et al. Formation and function of intracardiac valve cells in the *Drosophila*
612 heart. *J. Exp. Biol.* **220**, 1852–1863 (2017). https://doi.org/10.1242/jeb.156265

613 43. Barbosa, S. H., Godoy, R. S. M. & Martins, G. F. The basic plan of the adult heart is
614 conserved across different species of adult mosquitoes, but the morphology of heart-
615 associated tissues varies. *J. Med. Entomol.* **56**, 984–996 (2019).
616 https://doi.org/10.1093/jme/tjz045

617 44. Crossley, A. C. The ultrastructure and function of pericardial cells and other nephrocytes
618 in an insect: *Calliphora erythrocephala*. *Tissue Cell* **4**, 529–560 (1972).
619 https://doi.org/10.1016/S0040-8166(72)80029-6

620 45. Poiani, S. B. & Cruz-Landim, C. Histology and ultrastructure of pericardial cells of
621 *Scaptotrigona postica* Latreille (Hymenoptera, Apidae) in workers and queens of different
622 ages. *Micron* **38**, 766–770 (2007). https://doi.org/10.1016/j.micron.2006.11.008

623 46. Denholm, B. & Skaer, H. Bringing together components of the fly renal system. *Curr.*
624 *Opin. Genet. Dev.* **19**, 526–532 (2009). https://doi.org/10.1016/j.gde.2009.08.006

625

626 **Figure legends**

627 **Figure 1.** Whole-mount preparations of the heart of *Melipona quadrifasciata* foragers. A:
628 ventral view of the entire freshly dissected heart (h), no longer beating, appearing as a
629 translucent tube attached to the carcass. The organ has a dilation or bulb (B) at its posterior
630 portion. The rectangle indicates the valve corresponding to the region shown in "E", which
631 precedes the bulb. pc: pericardial cells forming a lateral cellular band surrounding the heart;
632 B: fixed and cleared bulb attached to the carcass, showing the longitudinal musculature (lm).
633 C: dorsal view of the bulb, showing circular muscle fibers (c) in an isolated heart post
634 fixation. D: ventral view of a freshly dissected and relaxed bulb, with the translucent blind-
635 ending region appearing as a circular opening (*) at the posterior end of the heart. E: narrow
636 region of a post-fixed heart, showing the transition between two cardiac chambers (ch),
637 forming a "<"-shaped structure. a–p: anteroposterior axis; arrow: transition between the bulb
638 and the anterior narrow region. lm: longitudinal cardiac muscle fibers; o: osti(um)a between
639 the two chambers.

640 **Figure 2.** Three-dimensional reconstructions generated from micro-computed tomography
641 images of the heart of a *Melipona quadrifasciata* forager, showing the three posterior-most
642 valves highlighted in different colors and the posterior bulb (B). A: lateral view; B: ventral
643 view; C: dorsal view. The inset shows the position of the heart (h) relative to abdominal
644 segments 4–7. asterisk: cardiomyocyte attachment line; ch: cardiac chambers; o: ostia.

645 **Figure 3.** Scanning electron micrographs of the heart and associated tissues (ventral views)
646 in *Melipona quadrifasciata* foragers. A: posterior portion of the heart showing the alary fibers

(a), which branch (b) and attach to the ventrolateral surfaces of the organ, forming the dorsal diaphragm (d). B: alary fibers (a) converging at a common attachment site on the integument (i). C: fracture exposing the lumen (L) of a narrower region of the heart. s: pericardial sinus delimited by dotted lines. D: posterior portion of the bulb showing its closed posterior end (*) and thin suspensory elements corresponding to putative extracellular matrix fibers (ef), which extend radially and connect the heart to the integument (i). E: transition (arrowhead) between two cardiac chambers (ch), corresponding to the region shown in Fig. 1E. Note the striated surface of the heart wall exposed after removal of the diaphragm. a–p: anteroposterior axis; b: branches of the alary fibers; pc: pericardial cells.

Figure 4. Scanning electron micrographs of the interior of the hearts of *Melipona quadrifasciata* foragers. A: ventral view of the longitudinally opened bulb, showing the lumen of its chambers (ch), followed by a narrowing of the muscular wall (w) in the regions corresponding to the ostia (o). a–p: anteroposterior axis;. B: lumen of a narrow portion of the heart. Arrow indicates the region of attachment between cardiomyocytes. C: transversely opened bulb, showing longitudinal muscle fibers (lm) on the ventral side. o: ostia. D: same bulb shown in C, showing the ostial lips (l), forming a valve, projecting into the bulb lumen (L). E: region corresponding to the closed posterior end of the bulb, showing longitudinal muscle fibers (lm). d–v: dorsoventral axis. F: anterior region of the bulb, showing the lumen narrowing toward the narrow portion of the heart. b: alary fiber branches; c: circular muscle fiber.

Figure 5. Whole-mount preparations of *Melipona quadrifasciata* hearts observed by confocal laser scanning microscopy (A–E) or fluorescence microscopy (F–G). A–B: hearts of virgin queens; C–G: hearts of foragers. Green: phalloidin-FITC (actin); red: TO-PRO-3 (DNA). A: posterior bulb showing longitudinal muscle fibers (lm) extending from its posterior end, narrowing toward the anterior region of the bulb's posterior chamber. a: alary fibers. B: narrow region of the heart showing a median line lacking phalloidin labeling (arrow), corresponding to the junction between the circular cardiomyocytes. pc: pericardial cells; n: nucleus of pericardial cells; N: cardiomyocyte nucleus. C: two lines lacking phalloidin-FITC labeling (arrows), corresponding to the junctions between cardiomyocytes. D: narrow region of the heart (h), corresponding to an intercameral region with a distinct

ostium (o). E: internal view of the transition region between the cardiac chambers shown in "D", revealing the ostial lips projecting into the cardiac lumen (L). F: second pair of ostia (o). G: anterior end of the heart near the thoracoabdominal junction, showing the beginning of the aorta (ao). a–p: anteroposterior axis; w: muscular wall.

Figure 6. Micro-computed tomography images of transverse sections of the heart and associated structures in a forager of *Melipona quadrifasciata*. The proportions of the structures were maintained for comparative purposes considering A-D. A, B: narrower region of the heart and a valve, respectively; C: dilated region of the antepenultimate cardiac chamber within the bulb; D: bulb valve (v). E, F: 3D reconstructions of the valve in the narrow cardiac region anterior to the bulb, shown in in posterior and anterior views. arrow: filiform projections extending from the distal ends of the ostial lips. G, H: 3D reconstructions of the bulb valve in proximal and distal views, respectively. d–v: dorsoventral axis; d: dorsal diaphragm; L: heart lumen; l: ostial lip; lm: longitudinal muscle; o: ostium; pc: pericardial cells; s: pericardial sinus.

Figure 7. Longitudinal semithin (A, B) and histological sections of the heart of a *Melipona quadrifasciata* forager stained with toluidine blue. A: bulb showing two dilated chambers (ch) separated by a valve composed of four ostial lips (l). Note the overlapping muscle layers (*) at the posterior end, which close the posterior end of the bulb. B: transition region between two chambers (ch) separated by the four ostial lips (l; valve) in a narrower portion of the heart. C: transition region between two chambers separated by the four ostial lips (l) of the bulb. D: detail of the muscle cells of two ostial lips in a bulb, showing cells that gradually taper from the base toward the distal end. E: detail of four ostial lips in a narrower portion of the heart. a–p: anteroposterior axis; L: heart lumen; n: nuclei of the ostial lip cells; o: ostia; pc: pericardial cells; w: muscular wall.

Figure 8. Histological sections of the heart of a *Melipona quadrifasciata* forager stained with toluidine blue. A: longitudinal section of the ventral surface of the bulb wall, showing circular muscle fibers (c) and longitudinally arranged cardiomyocytes (lm) in the ventral region. a–p: anteroposterior axis. B: longitudinal section of the dorsal surface of the bulb wall, showing multinucleated cardiomyocytes converging at a point of contact (arrow) between them in the median region of the bulb. C: Transverse section of a bulb showing two indented regions

(arrows) representing junctions between cardiomyocytes. Longitudinal muscle fibers (lm) are visible in the ventral region and are external to the circular fibers. a: alary fiber. D: transverse section of a narrow region of the heart showing the point of union between the cardiomyocytes (arrows). d–v: dorsoventral axis; L: heart lumen; n: nuclei; pc: pericardial cells; w: heart wall.

Figure 9. Transmission electron micrographs of the cardiac musculature of a *Melipona quadrifasciata* forager. A: general organization of the thick muscular wall of the bulb, showing mitochondria (m) and Z-lines (z). B: distal region of two ostial lips of the bulb, showing thin cells with evident contractile organization, as indicated by the presence of sarcomeres (s) between two Z-lines. L: cardiac lumen. C: detail of a region of an ostial lip cell showing the typical organization of the contractile cytoskeleton, the nucleus (n), endoplasmic reticulum (e), and a Z-line.

Figure 10. Sections of the heart bulb of a *Melipona quadrifasciata* forager. A, B: histological sections stained with toluidine blue. A: longitudinal section of the thick muscular wall (w) of the bulb and the dorsal diaphragm (d), which extends along ventral surface of the heart. i: integument. B: Transverse section of the bulb showing the diaphragm (d), formed by alary fibers (a), which branch (b) beneath the bulb and extend laterally along its sides. C: Transmission electron micrograph showing the cellular structure of the alary fiber branches that form the diaphragm adjacent to the heart wall (w). bl: basal lamina; d–v: dorsoventral axis; ef: extracellular matrix fibers; L: heart lumen; n: nucleus; pc: pericardial cells.

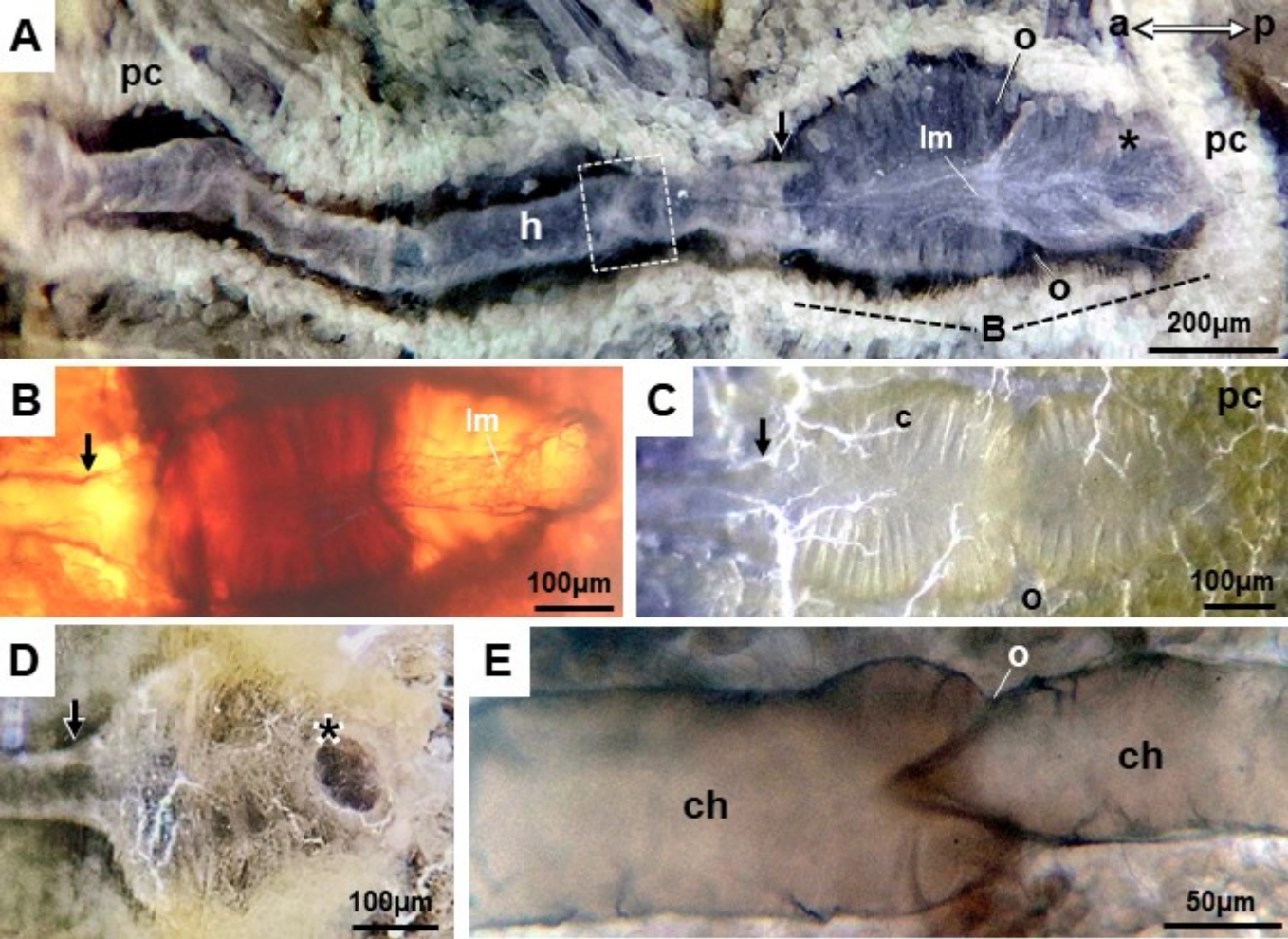
Figure 11. Pericardial cells (pc) in *Melipona quadrifasciata*. A: clusters of pericardial cells adjacent to the heart (h) of a queen, arranged in linear groups forming a continuous cellular mass physically associated with the heart (h) and alar fibers (a), as observed by confocal laser microscopy. Green: phalloidin-FITC (actin); red: TO-PRO-3 (DNA). B: transmission electron micrograph of a group of pericardial cells in a forager, showing several surface invaginations (i) and organelle-like structures associated with endocytosis (*). is: intercellular space; bl: basal lamina; n: nucleus of pericardial cells; N: nucleolus.

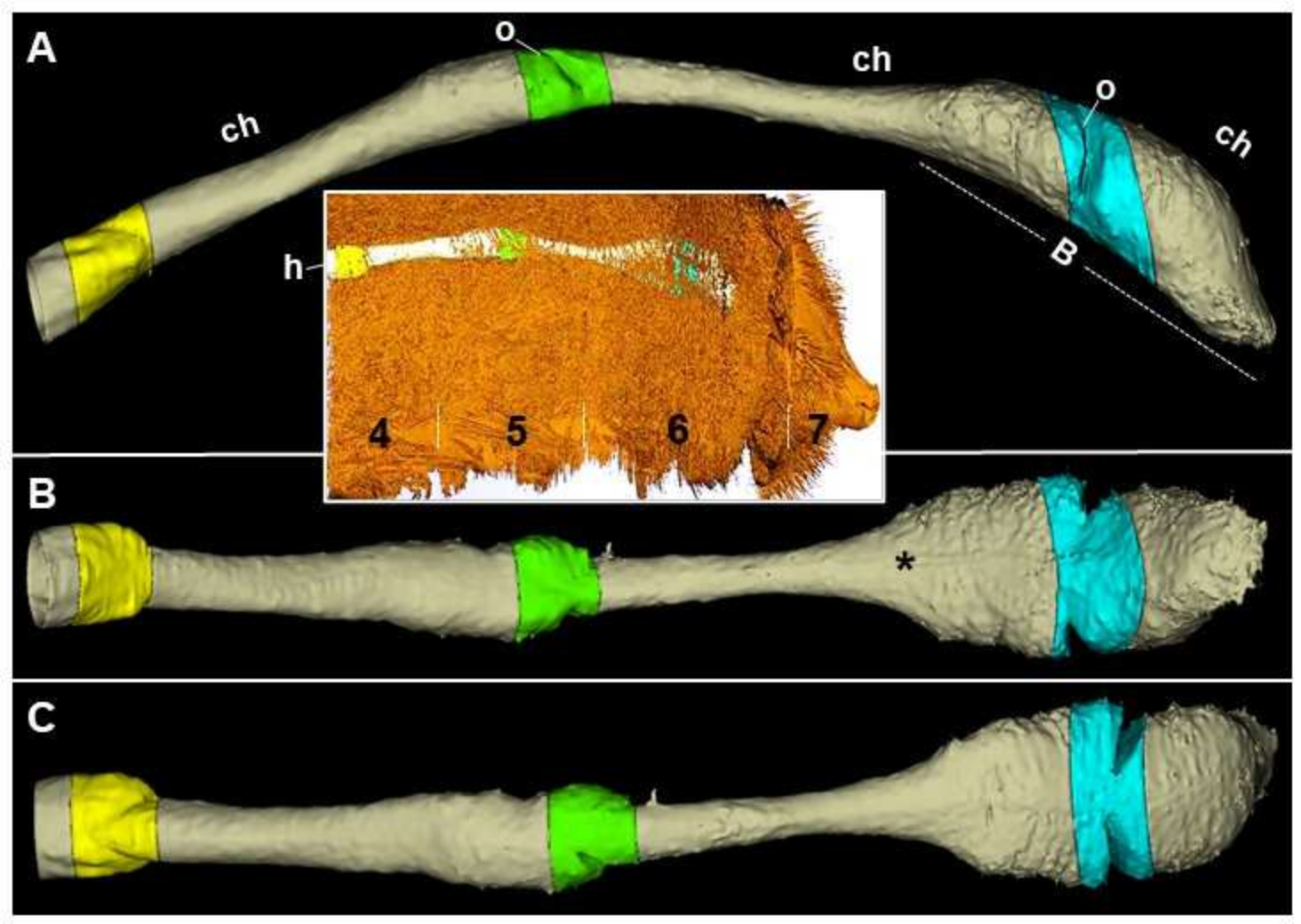
Supplementary Video 1. Ventral view of the heart of a forager of *Melipona quadrifasciata*, showing the bulb, the successive anterior cardiac chambers, and the five pairs of ostia. The organ was stained with phalloidin-FITC.

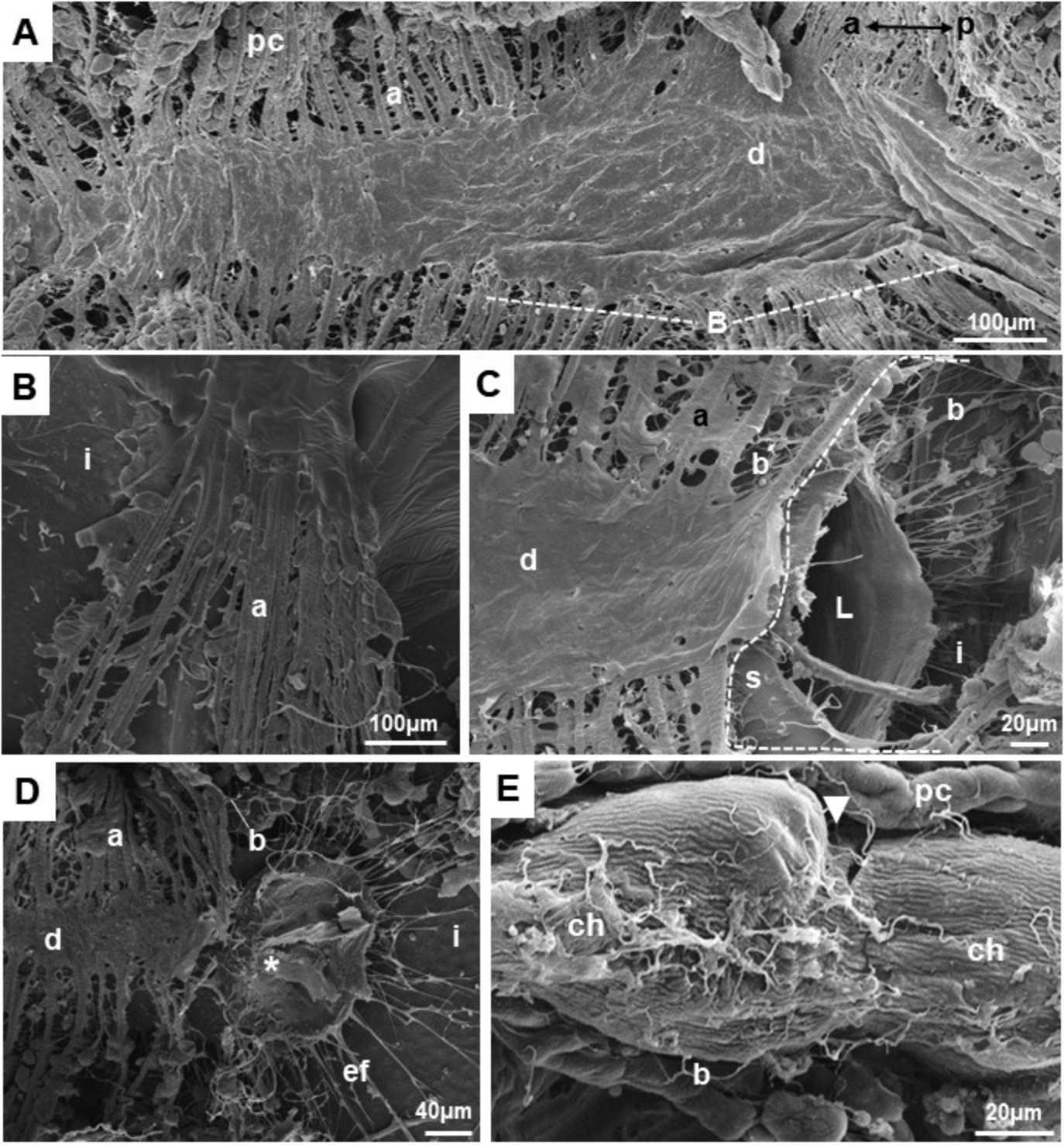
Supplementary Video 2. Three-dimensional reconstruction from micro-computed tomography data showing external and internal views of the posterior region of the heart in a forager of Melipona quadrifasciata, highlighting the three posterior-most valves.

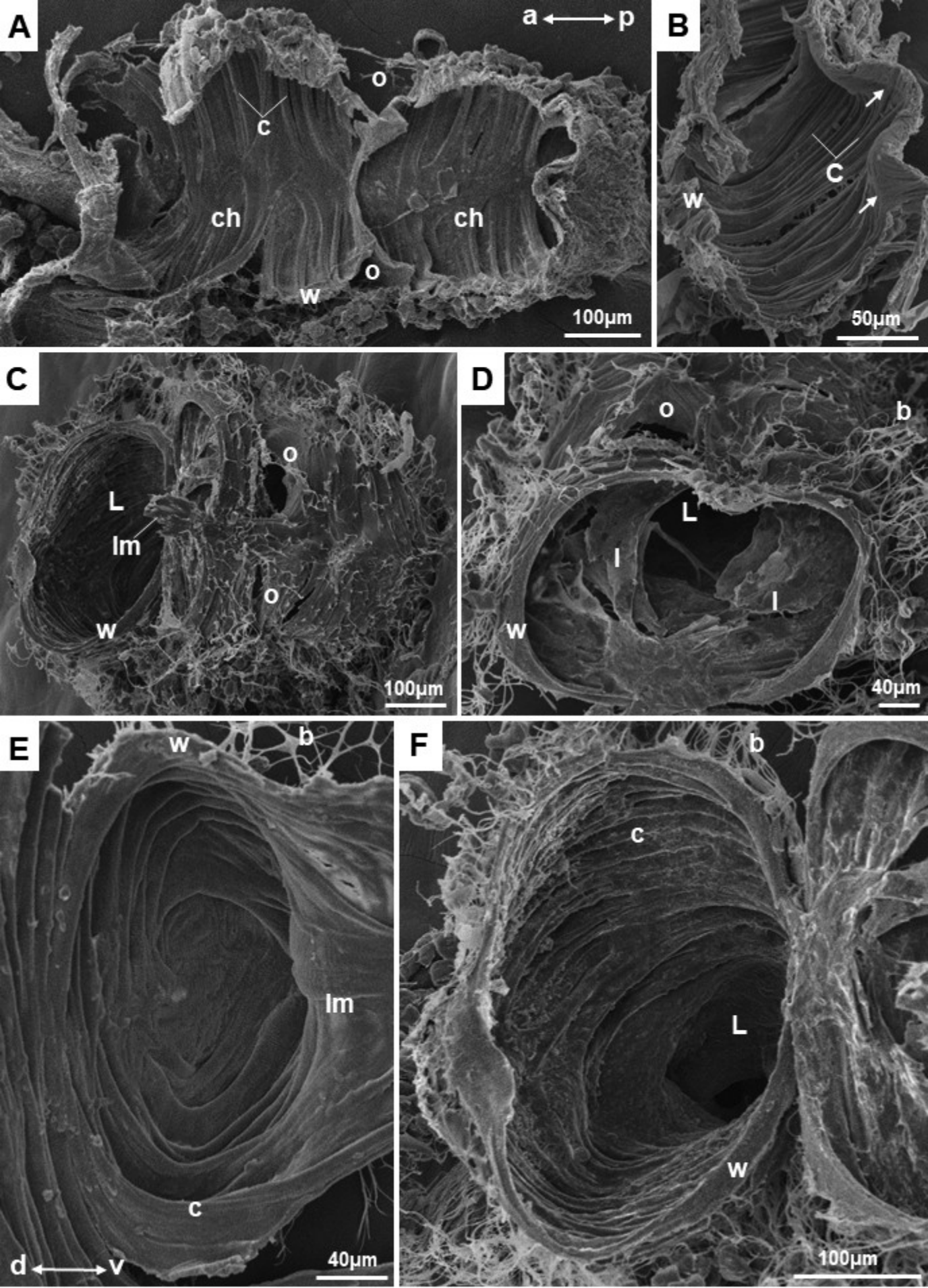
Supplementary Video 3. Three-dimensional segmentation of micro-computed tomography data showing sequential transverse views of the posterior region of heart and associated structures along its length in a forager of *Melipona quadrifasciata*.

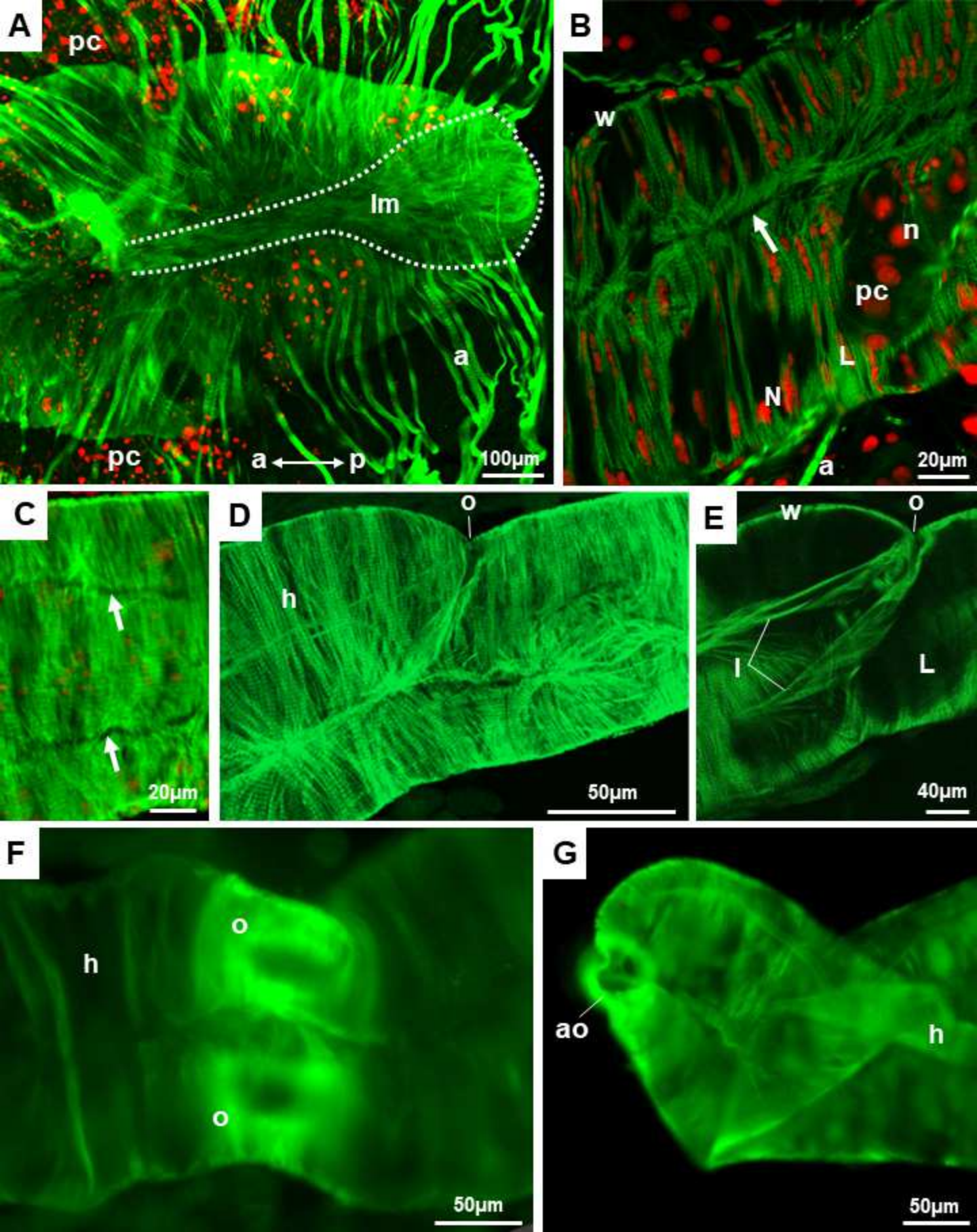
Supplementary Video 4. Beating of the posterior region of the freshly dissected heart of a forager of *Melipona quadrifasciata*.

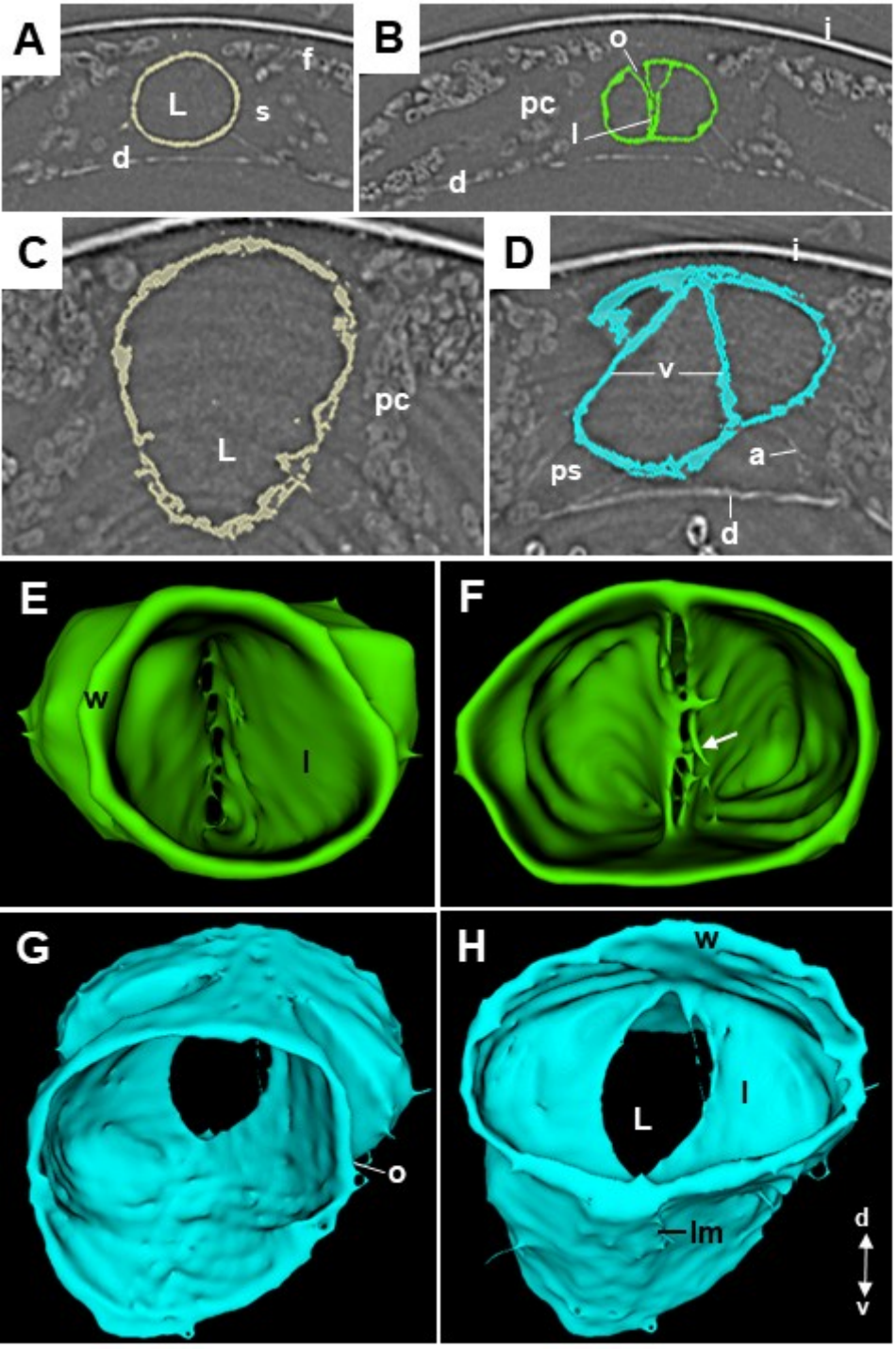

A
pc
a
p
o
lm
*
pc
h
o
B
200µm
B
lm
100µm
C
c
pc
o
100µm
D
*
100µm
E
o
ch
ch
50µm

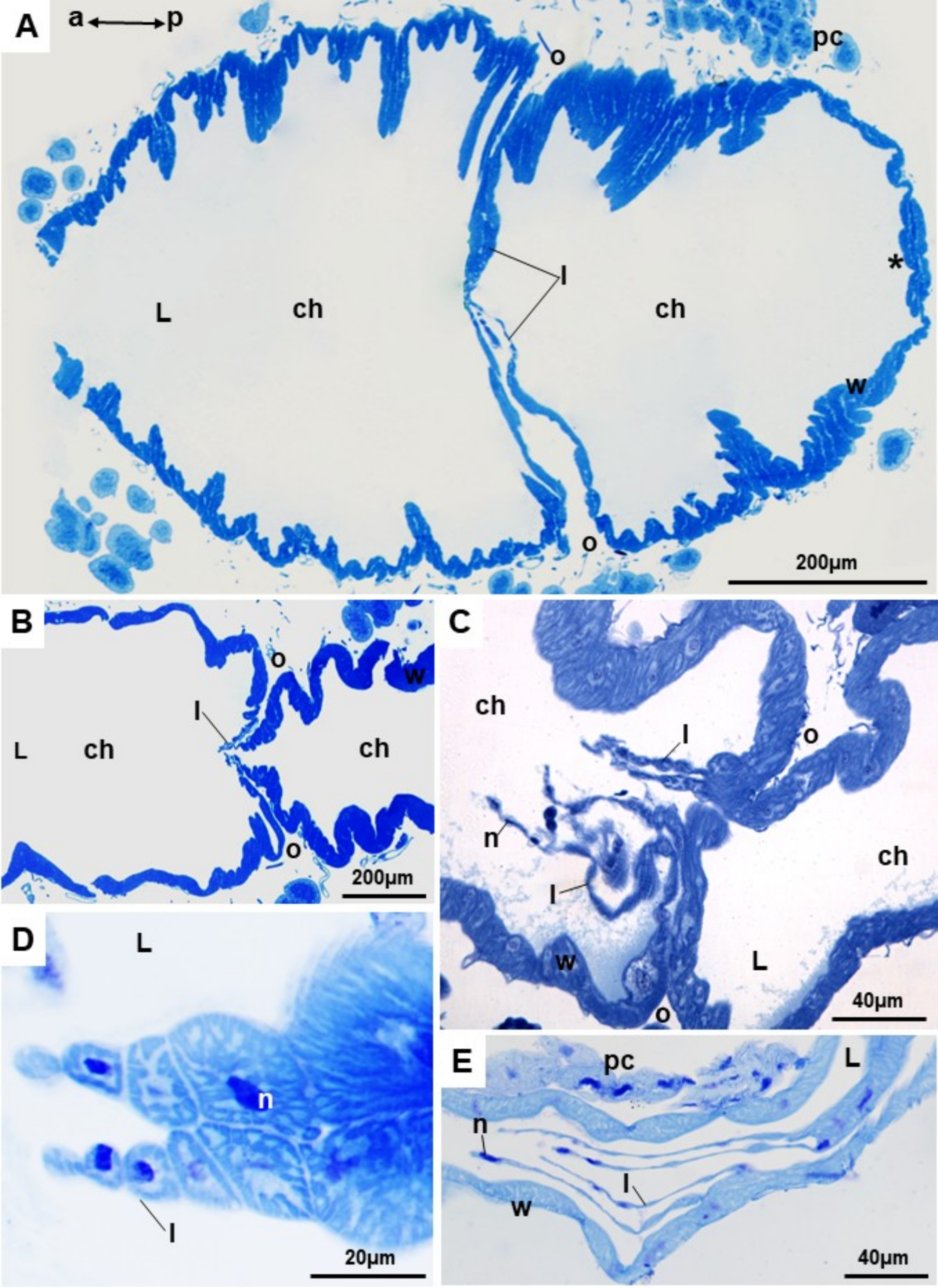

A
o
ch
ch
o
ch
h
B
4
5
6
7
B
*
C

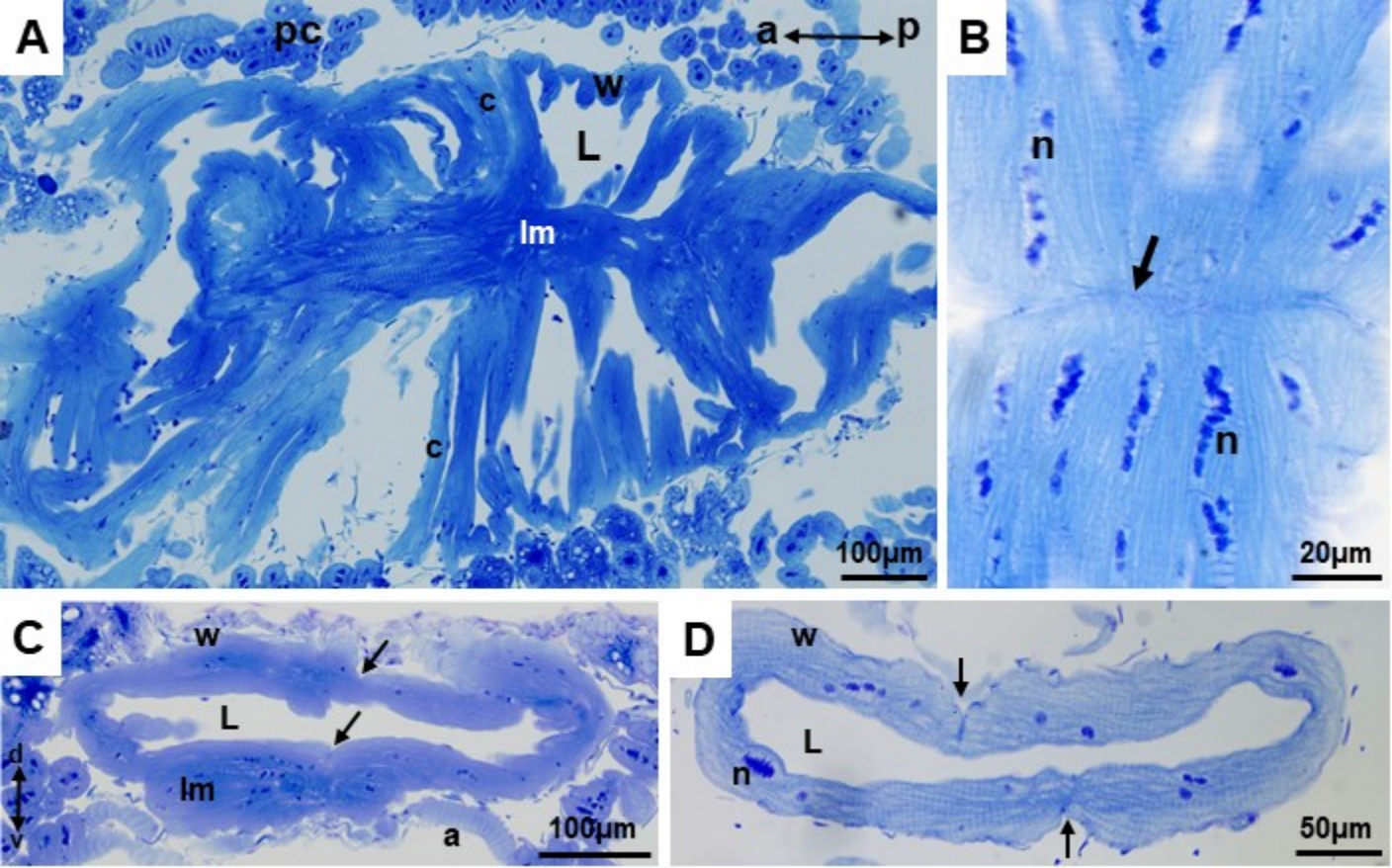

A
pc
a
a
p
d
B
100µm
B
i
a
100µm
C
a
b
b
d
L
i
s
20µm
D
a
b
d
i
*
ef
40µm
E
pc
ch
ch
b
20µm

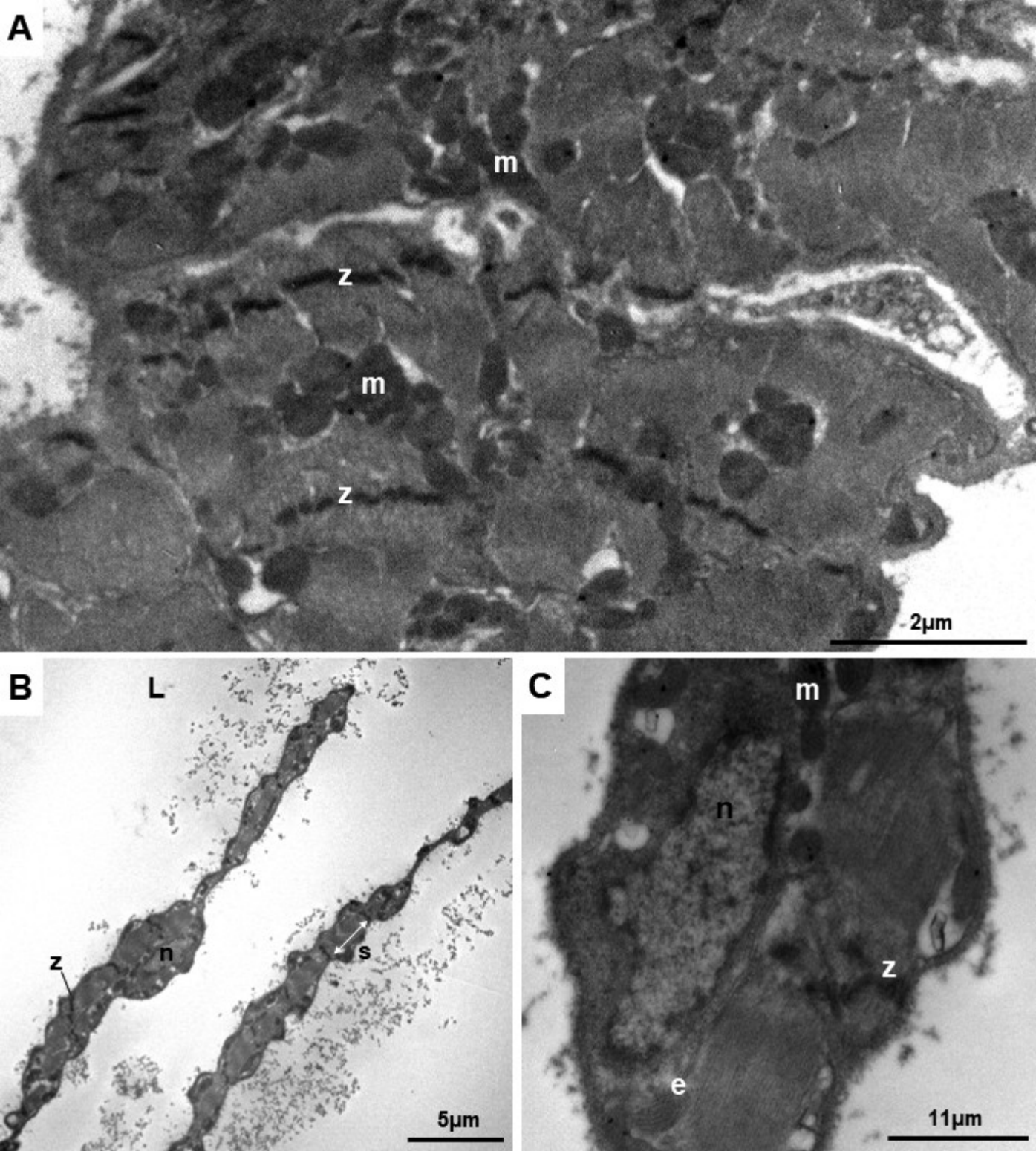

A
a
p
o
c
ch
ch
o
w
100µm
B
C
w
50µm
C
o
L
lm
o
w
100µm
D
o
b
L
l
l
w
40µm
E
w
b
lm
c
d
v
40µm
F
b
c
L
w
100µm

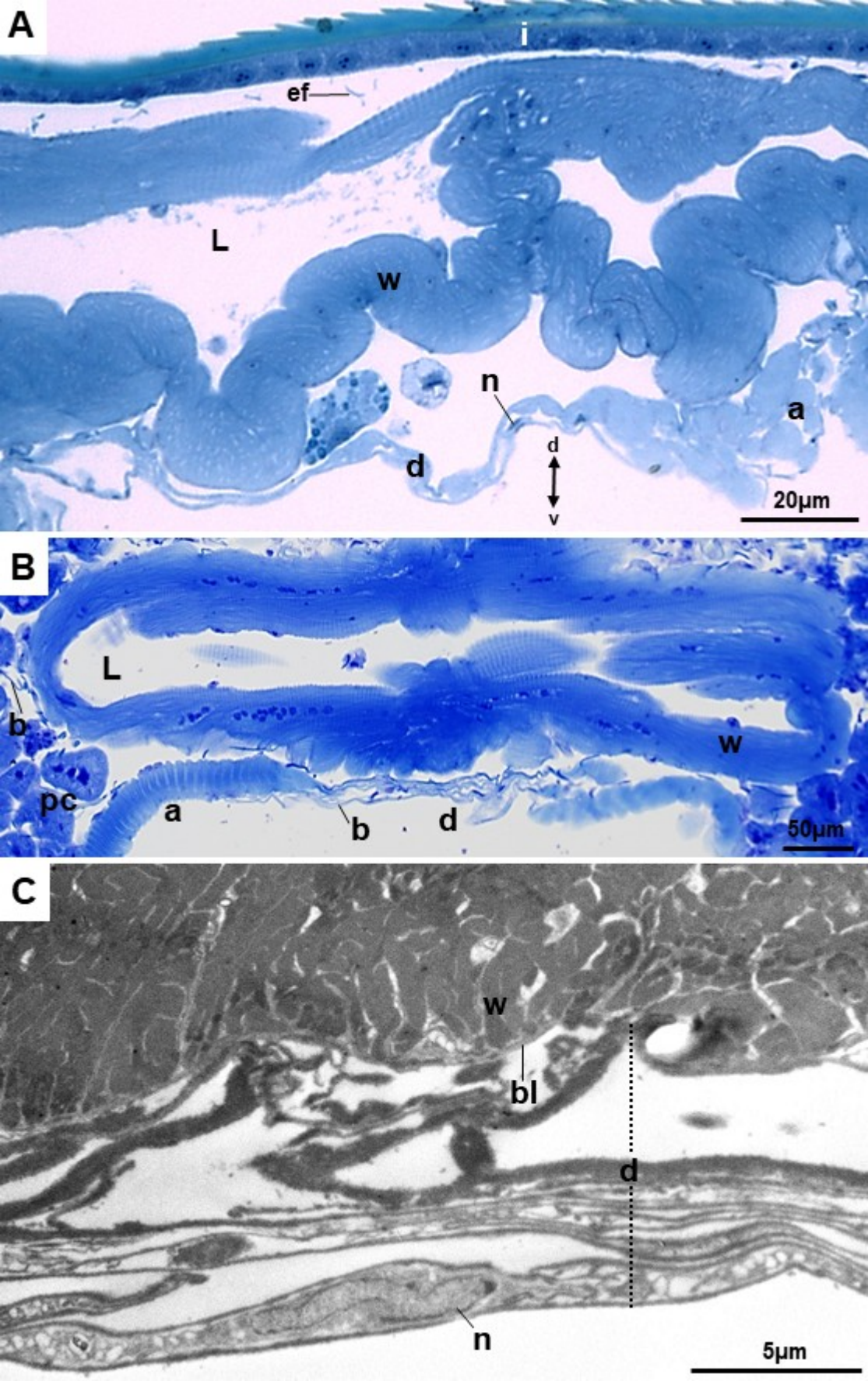

A
pc
lm
a
pc
a ↔ p
100µm
B
w
n
pc
L
N
a
20µm
C
20µm
D
o
h
50µm
E
w
o
l
L
40µm
F
h
o
o
50µm
G
ao
h
50µm

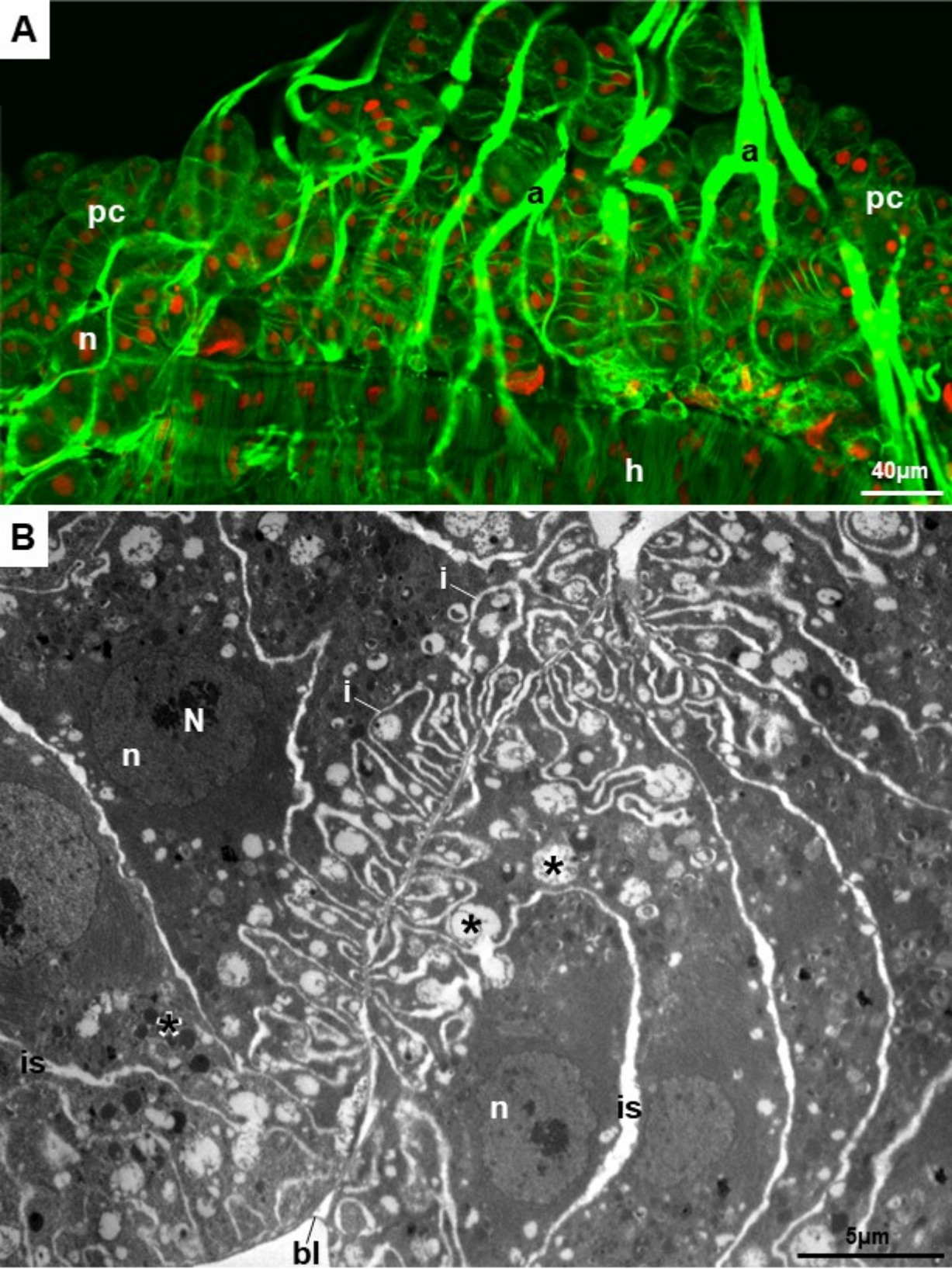

A
L
f
s
d
B
o
i
pc
l
d
C
pc
L
D
i
v
ps
a
d
E
w
l
F
G
o
H
w
L
l
lm
d
v


A
a
p
pc
o
l
*
L
ch
ch
w
o
200µm
B
o
w
l
L
ch
ch
o
200µm
C
ch
l
o
n
ch
l
w
L
o
40µm
D
L
n
l
20µm
E
pc
L
n
l
w
40µm


A
pc
a
p
c
w
L
lm
c
100μm
B
n
n
20μm
C
w
L
lm
d
v
a
100μm
D
w
L
n
50μm


A
m
z
m
z
2µm
B
L
z
n
s
5µm
C
m
n
z
e
11µm


A
i
ef
L
w
n
a
d
d
v
20µm
B
L
b
w
pc
a
b
d
50µm
C
w
bl
d
n
5µm


A
pc
n
a
a
pc
h
40μm
B
i
i
N
n
*
*
*
is
n
is
bl
5μm

Supplementary Files

This is a list of supplementary files associated with this preprint. Click to download.

- Sup.Video1.mp4
- Sup.Video2.mp4
- Sup.Video4.mp4
- Sup.Vdeo3.mp4